Performance of GeoMx CTA and WTA, high-plex, spatial gene expression profiling tools

AUTHORS: Kristina Sorg[1], JingJing Gong[1], Stephanie Zimmerman[1], Robin Fropf[1], Anna Pavenko[1], Jason Yeon[1], Maddy Griswold[1], Karen Nguyen[1], Zoey Zhou[1], Zach Norgaard[1], Chris Merritt[1], Margaret Hoang[1], Michael D Rhodes[1], Yan Liang[1], Sarah E Warren[1], Jason W Reeves[1], Joseph Beechem[1].

1.NanoString Technologies, Inc., Seattle, Washington, USA

Introduction

Pathological assessment of tissues frequently requires rare or limited tissue samples to be exhausted when testing multiple biomarkers. High-plex profiling of gene expression under bulk or single-cell analysis provides rich contextual information but consumes large fractions of tissues and lacks spatial context from key morphological features. As such, direct interrogation tools are needed to enable characterization of localized transcriptomic changes in discrete tissues while preserving additional tissues for testing. Here, we demonstrate the capabilities of the GeoMx™ Digital Spatial Profiling (DSP) platform to robustly quantify high-plex RNA expression data from single, 5 um Formalin-Fixed Paraffin Embedded (FFPE) sections, capturing genome-wide expression patterns in spatially resolved locations throughout tissues.

To test the sensitivity and specificity of DSP on well controlled tissues, we profiled cells lines which have known expression profiles. In parallel, we examined expression patterns from FFPE normal tissues to demonstrate the capabilities of DSP to profile across diverse tissue types. To confirm that DSP accurately captures the expression profiles relevant to these tissues and cell lines, we compared DSP data against publicly available RNAseq data from matched and unmatched cell lines and tissue types.

Materials and Methods

Experimental design

Panel: Using DSP, we profiled the gene expression in FFPE cell lines and in regions-of-interest (ROIs) within normal tissues. We used two DSP panels. The Cancer Transcriptome Atlas (CTA) targets 1,800+ genes involved in immune response, tumor biology, and the microenvironment. The Whole Transcriptome Atlas (WTA) currently has 16,000+ protein coding targets and is building toward 18,000+.

Samples: With CTA, we profiled 11 FFPE cell lines, collecting from 200 um^2 diameter (31,416 um^2) ROIs. With WTA, we profiled 7 FFPE cell lines, collecting from 250 um diameter (49,087 um^2) ROIs. We collected samples in duplicate and took the mean of counts for each target. Using both panels, we also profiled normal tissues from an FFPE tissue microarray (TMA), collecting 267 ROIs spanning 8 tissue types and 74 donors. ROIs range from 1,922 to 281,629 um^2 and are mostly circles. Some ROIs encompass distinct morphological regions including kidney tubules or glomeruli and spleen red pulp or white pulp.

Analysis: We compared DSP data to public RNAseq data, comparing cell lines to the Cancer Cell Line Encyclopedia (CCLE) (Ghandi et al., 2019), which contains 1,019 unfixed cell lines, and normal tissues to the Genotype-Tissue Expression (GTEx) Project (Carithers et al., 2015), which contains 17,000+ samples spanning 30 tissue types. We calculated correlation, sensitivity, and specificity of cell lines relative to RNAseq, as well as rate of accurate classification when compared to matched and unmatched cell lines. In normal tissues, we again looked at a rate of accurate classification, this time by tissue type. We also looked within tissue type, at gene expression and cell proportions, to compare distinct ROIs within spleen. All correlations are Pearson's, cell proportions are calculated with SpatialDecon (Danaher et al., 2020 preprint).

Workflow

RNA-binding oligos coupled to unique RNA identifiers

DSP probes are RNA-binding oligos coupled to photocleavable oligo tags, which contain unique RNA identification codes.

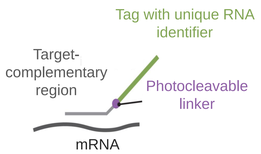

ROIs collected from micrometer scale regions of interest in FFPE tissues

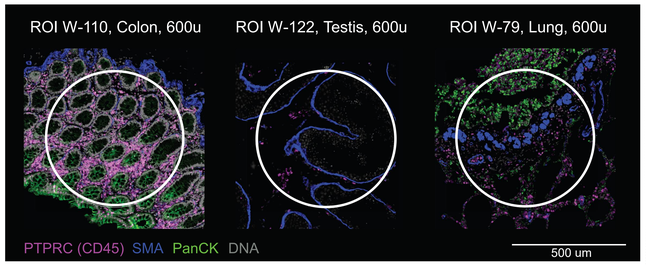

GeoMX DSP workflow

With an in-situ hybridization protocol, probes hybridize to mRNA in 5 um tissues sections. Fluorescent antibodies, applied with standard immunohistochemistry methods, guide ROI selection at 20X on a DSP microscope. UV light, directed by dual digital micromirror devices, releases the photocleavable tags from ROIs. Cleaved tags contain RNA identifiers, two primer binding sites, and a unique molecular identifier (UMI). After collection of tags, PCR adds unique dual indices, indexing each ROI. Samples are pooled and sequenced with next-generation sequencing (NGS). A custom DSP NGS pipeline processes reads into counts, using the RNA identifier to call genes and the UMI to account for PCR bias.

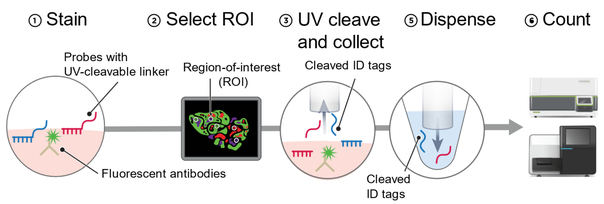

Results

Benchmarking DSP against RNAseq

DSP was performed on FFPE samples, known to have degraded RNA relative to unfixed tissues. CCLE RNAseq was performed on unfixed tissues and with larger RNA inputs per sample. Relative to CCLE RNAseq data, CTA and WTA sensitivity is .66 and .71 and specificity is 1.00 and .98, respectively. Rate of accurate classification is 10/11 in CTA and 7/7 in WTA (right), with average correlations of .91 in each panel (below, data above detection shown). The one misclassified line, HEL, misclassifies as HEL9217. HEL and HEL9217 are from the same parent cell line; within the CCLE data, they correlate well (r = 0.97).

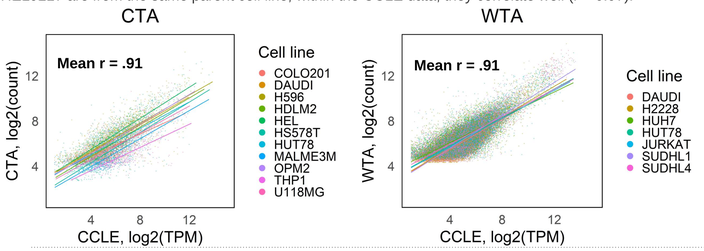

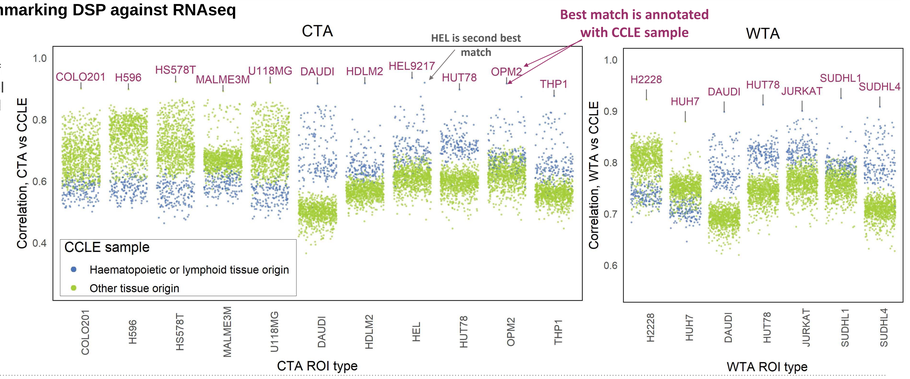

Normal tissue versus bulk RNAseq

Ninety-one of 113 CTA ROIs (81%) and 121 of 154 WTA ROIs (79%) ROIs correlate better with matched tissue types than unmatched tissue types in the GTEx RNAseq data. We made comparisons across individual, sex, and age, only noting tissue type. GTEx samples are bulk tissue samples while DSP ROIs are from discrete, micrometer scale regions within tissues, in some cases containing specific morphological features such as single glomeruli.

Correlation of ROIs to tissue-type-matched and tissue-type-unmatched RNAseq samples

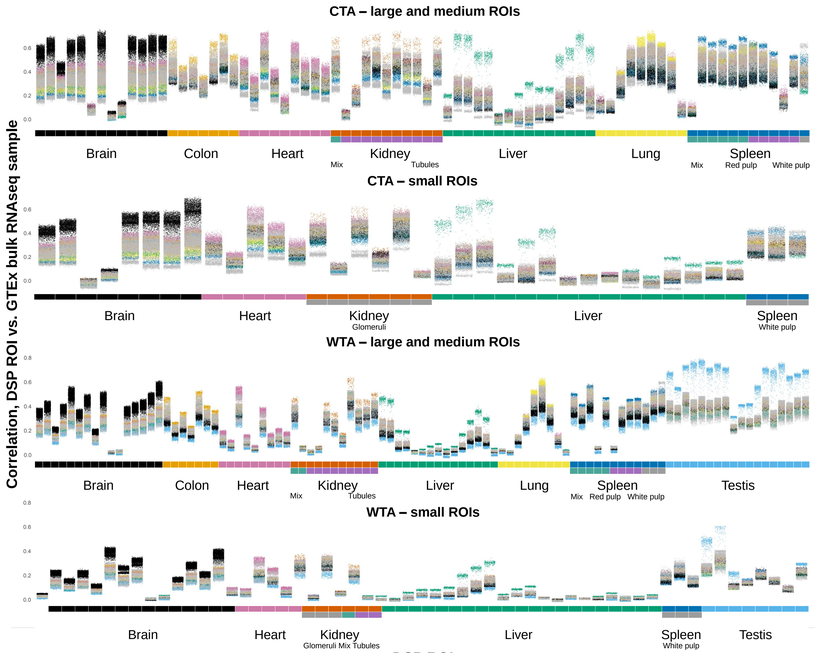

GTEx bulk RNAseq tissue type

Adipose Tissue, Adrenal Gland, Bladder, Blood, Blood Vessel, Brain, Breast, Cervix Uteri, Colon, Esophagus, Fallopian Tube, Heart, Kidney, Liver, Lung, Muscle, Nerve, Ovary, Pancreas, Pituitary, Prostate, Salivary Gland, Skin, Small Intestine, Spleen, Stomach, Testis, Thyroid, Uterus, Vagina

Adding spatial context to spleen profiles

Spleen ROIs are red pulp, white pulp, or mixed. White pulp is a lymphoid tissue containing B cell compartments. Red pulp, which filters passing blood, consists of more connective tissue. Across CTA and WTA, 8 of 11 mixed ROIs, but only 4 of 19 red or white pulp ROIs, corelate best with bulk spleen samples from GTEx RNAseq data, indicating spleen ROIs may have gene expression profiles with rich spatial information. With CTA, we find the white pulp ROIs to be plentiful in B cells, as expected, in contrast to red pulp ROIs, which contain more macrophages and monocytes.

Spleen ROIs from red or white pulp

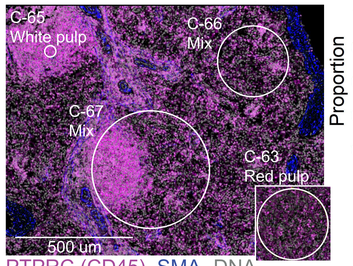

Cell type profiles from CTA data

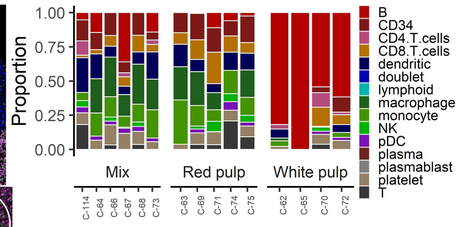

Gene expression

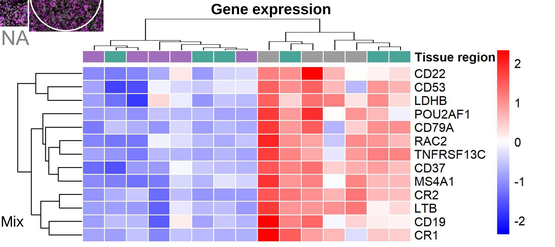

CD19, MS4A1, and CD79A are B cell markers. CD22, CD37, CR1, CR2, LTB, POU2FA1, and TNFRSF13C are expressed by or associated with B cells. These and a few others are high in white pulp ROIs.

Conclusions

CTA and WTA enable transcriptome-scale spatially resolved profiling to enable molecular characterization of single FFPE tissue sections, creating a workflow that helps resolve the need to preserve these tissues while also deeply characterizing their morphology, gene expression, and interplay of the two.

Carithers LJ, et al. A Novel Approach to High-Quality Postmortem Tissue Procurement: The GTEx Project. Biopreserv Biobank. 2015 Oct;13(5):311-9. doi: 10.1089/bio.2015.0032. PMID: 26484571; PMCID: PMC4675181.

Danaher P, et al. Advances in mixed cell deconvolution enable quantification of cell types in spatially-resolved gene expression data. Preprint at https://www.biorxiv.org/content/10.1101/2020.08.04.235168v1. https://github.com/Nanostring-Biostats/SpatialDecon

Ghandi M, et al. Next-generation characterization of the Cancer Cell Line Encyclopedia. Nature. 2019 May;569(7757):503-508. doi: 10.1038/s41586-019-1186-3. Epub 2019 May 8. PMID: 31068700; PMCID: PMC6697103.